frontiers in PHYSIOLOGY

ORIGINAL RESEARCH ARTICLE
published: 04 May 2012
doi: 10.3389/fphys.2012.00120

Osmotic gradients induce bio-reminiscent morphological transformations in giant unilamellar vesicles

Kamila Oglęcka[1], Jeremy Sanborn[2], Atul N. Parikh[2,3] and Rachel S. Kraut[1]*

[1] *Division of Molecular Genetics and Cell Biology, School of Biological Sciences, Nanyang Technological University, Singapore*
[2] *Departments of Biomedical Engineering, Chemical Engineering and Materials Science, University of California, Davis, CA, USA*
[3] *Center for Biomimetic Sensor Science, School of Materials Science and Engineering, Nanyang Technological University, Singapore*

Edited by:
Ali Mobasheri, The University of Nottingham, UK

Reviewed by:
Luis M. S. Loura, University of Coimbra, Portugal
Habibeh Khoshbouei, Meharry Medical College, USA

***Correspondence:**
Rachel S. Kraut, Division of Cell and Molecular Biology, School of Biological Sciences, Nanyang Technological University, 60 Nanyang Drive, Singapore 637551.
e-mail: rskraut@ntu.edu.sg

We report observations of large-scale, in-plane and out-of-plane membrane deformations in giant uni- and multilamellar vesicles composed of binary and ternary lipid mixtures in the presence of net transvesicular osmotic gradients. The lipid mixtures we examined consisted of binary mixtures of DOPC and DPPC lipids and ternary mixtures comprising POPC, sphingomyelin and cholesterol over a range of compositions – both of which produce co-existing phases for selected ranges of compositions at room temperature under thermodynamic equilibrium. In the presence of net osmotic gradients, we find that the in-plane phase separation potential of these mixtures is non-trivially altered and a variety of out-of-plane morphological remodeling events occur. The repertoire of membrane deformations we observe display striking resemblance to their biological counterparts in live cells encompassing vesiculation, membrane fission and fusion, tubulation and pearling, as well as expulsion of entrapped vesicles from multicompartmental giant unilamellar vesicles through large, self-healing transient pores. These observations suggest that the forces introduced by simple osmotic gradients across membrane boundaries could act as a trigger for shape-dependent membrane and vesicle trafficking activities. We speculate that such coupling of osmotic gradients with membrane properties might have provided lipid-mediated mechanisms to compensate for osmotic stress during the early evolution of membrane compartmentalization in the absence of osmoregulatory protein machinery.

Keywords: osmotic gradients, giant unilamellar vesicles, phase separation, vesiculation, membrane dynamics

INTRODUCTION

Giant unilamellar vesicles (GUVs), mimicking the simplest cell-like structures, consist of topologically closed, two-dimensionally fluid elastic shells, which isolate their encapsulated aqueous core from the surrounding bulk (Walde et al., 2010). They provide a basic structural motif for biological compartmentalization allowing cells and organelles to maintain physically isolated, distinct aqueous environments in close proximity to each other. The membranous shell itself consists of two apposed monomolecular leaflets stabilized by a combination of electrostatic, van der Waals, and entropic "hydrophobic" forces. At the macroscopic level, membranes display a unique combination of elastic properties (Evans and Needham, 1987; Needham and Nunn, 1990; Bloom et al., 1991), which include large volume compressibility ($\sim 10^9$ to 10^{10} N/m^2) and area expansion (10^2 to 10^3 mN/m) moduli, and low bending rigidities (10^{-19} Nm). As a result, the vesicular membrane is (1) highly resistant to compression, (2) tolerates only a limited expansion in surface area ($\sim$2–10%) prior to lysis at lateral tensions corresponding to 3–30 mN/m, and (3) exhibits a spectacularly broad range of bending-dominated shape fluctuations (e.g., flickering) at thermal equilibrium under constraints of fixed surface area and fixed volume (Lipowsky, 1991; Seifert, 1997), which give rise to a variety of shape transitions (Baumgart et al., 2003).

Weak external perturbations suffice to lift the equilibrium constraints of constant area to volume ratio, rendering membranes susceptible to an even broader range of large-scale morphological remodeling. For example, elevating vesicle temperature in certain cases induces a so-called budding transition where an initially spherical vesicle transforms – via well-resolved prolate- and pear-shaped intermediates – into one with a daughter bud, which remains connected to the reduced mother vesicle by a narrow neck (Berndl et al., 1990; Käs and Sackmann, 1991). In other examples, spherical vesicles assume oblate-shaped intermediates upon heating, ultimately transforming into more exotic discocytes and stomatocytes (Berndl et al., 1990). More recently, non-equilibrium transitions, such as those induced by pinching the membrane with optical tweezers, have been reported. The tweezer-induced tension drives the formation of cylindrical protrusions from the parent vesicle, which subsequently transform into a string of daughter vesicles, forming a "a pearl necklace" (Bar-Ziv and Moses, 1994). A key requirement for these (and other related) bending-mediated shape transformations is the generation of membrane asymmetry, which stems from a difference in area between the inner and outer leaflets of the bilayer (Döbereiner et al., 1997). Because lipid leaflets of the bilayer membrane are practically incompressible, any difference in the area of the two leaflets gives rise to bending-mediated deformations (Miao et al., 1994; Seifert, 1997). For instance, temperature-induced transitions result from subtle differences in thermal expansivities of the two leaflets. This in turn produces an area mismatch between the leaflets giving rise

to the variety of predictable shape transitions summarized above. This extreme responsiveness of the closed lipid vesicles to external perturbations is invoked as a basis for the morphology or shape-dependent physiological activity in living cells (Berndl et al., 1990; Frolov et al., 2011).

A pervasive source of external perturbations is the presence of solutes in the aqueous ambient. Although water equilibrates over millisecond time scales across vesicular membranes with sufficiently fast kinetics (10^{-2} to 10^{-3} cm^3/cm^2 s), passive permeation of solutes (e.g., protons, ions, and neutral molecules) is strongly hindered (Deamer and Bramhall, 1986). As a result, gradients of pH, ionic strength and osmotic pressure arise between the compartmentalized volume and the surrounding bulk. The existence of such concentration gradients can become a source of external perturbation driving biologically relevant membrane deformations. For example, a gradient of proton concentration across the vesicular membrane can preferentially neutralize anionic lipids (e.g., phosphatidylserine or cardiolipin) in the leaflet facing the acidic aqueous phase. This in turn weakens the electrostatic repulsion between the headgroups of these lipids and decreases their effective area, generating area asymmetry. Acidic vesicular interiors (or exteriors) thus can lead to inward invagination (or outward protrusions), or the converse under basic conditions (Khalifat et al., 2008; Fournier et al., 2009).

In this same vein, osmotically driven water flow, from a bulk containing a low solute concentration to the vesicular compartment with a higher solute concentration, can provide an energetic input that can be transduced into mechanical membrane deformations. Specifically, water influx resulting from exposure to hypotonic media results in macroscopic swelling of GUVs. In the limiting case, when osmotically inflated vesicles stretch the membrane beyond its lysis tension, they rupture, or in certain cases, form transient pores through which solutes escape (Koslov and Markin, 1984; Zhelev and Needham, 1993; Sandre et al., 1999). Such pore formation provides a mechanism by which intravesicular pressure can be released and thus might have provided protection against osmotic bursting in a hypothetical primordial proto-cell devoid of specialized membrane proteins (Budin and Szostak, 2011). In modern cells, however, mechanosensitive channel proteins have evolved to help regulate osmotic gradients by coupling membrane permeability to membrane tension (Martinac et al., 1987; Yang and Sachs, 1989).

While these limiting case scenarios have been extensively studied over the past several decades, the coupling of morphology of membranes, especially multicomponent ones, with milder osmotic gradients of the kind that might occur in living cells, has received much less attention. Previously, Boroske et al. (1981) reported that osmotically induced water efflux from vesicular confinements of simple zwitterionic lipid bilayers gives rise to a continuous, monotonic shrinkage of thin-walled (probably unilamellar) GUVs. In thick-walled or multilamellar vesicles, the authors demonstrate the appearance of tubular protrusions, which they suggest might herald incipient daughter vesicle generation by fission. Such complete fission of giant vesicles has been experimentally demonstrated for multicomponent lipid mixtures containing sterols under osmotic deflation (Döbereiner et al., 1993; Bacia et al., 2005).

In this study, we report observations of a diversity of vesicular behaviors obtained in single populations of multicomponent GUVs subjected to osmotic gradients. Osmotic gradients were generated using gradients of sucrose (or galactose) concentration. We used two distinct classes of lipid mixtures: (1) Prototypical raft-forming ternary lipid mixtures consisting of cholesterol, sphingomyelin and POPC, and (2) binary mixtures consisting of the higher-melting gel-phase DPPC (T_m, 41°C) mixed with the fluid DOPC (T_m, −2°C). Amongst the observed morphological changes, our findings include a qualitatively significant modulation of in-plane phase separation and a dramatic variety of out-of-plane deformations, with the most dynamic structures appearing in fluid L_o/L_d mixtures. Specifically, we observe (1) vesicular fission and fusion; (2) fingering, tubulation and pearling; (3) involution and expulsion of internalized vesicles. Implications of these results for certain morphological behaviors of biological and model membranes are discussed.

MATERIALS AND METHODS

MATERIALS

DOPC (1,2-dioleoyl-*sn*-glycero-3-phosphocholine), DPPC (1,2-dipalmitoyl-*sn*-glycero-3-phosphocholine), GM1 (monosialotetrahexosylganglioside), sphingomyelin (chicken egg) and cholesterol were obtained from Carbosynth, Berkshire, UK. POPC (1-palmitoyl-2-oleoyl-*sn*-glycero-3-phosphocholine), Egg PC 99%, Rhodamine-DPPE (lissamine rhodamine B 1,2-dihexadecanoyl-*sn*-glycero-3-phosphoethanolamine, triethylammonium salt; also abbreviated Rhodamine-DHPE) and Rhodamine B DOPE (lissamine rhodamine B 1,2-dioleoyl-*sn*-glycero-3-phosphoethanolamine) were from Avanti Polar Lipids, AL, USA. Fluorescein was acquired from Invitrogen, Carlsbad, CA, USA. Atto488-DPPE was purchased from Atto Tec, Siegen, Germany, while the lipid analog 5-TAMRA-J116S was a gift from Gary Jennings at JADO-tech, Dresden, Germany. Sucrose was from USB Corporation, Cleveland, OH, USA; galactose was a gift from Philip Chan, NTU, Singapore. Laurdan (6-dodecanoyl-2-dimethylaminonaphthalene) was purchased from Molecular probes, Invitrogen. All buffer chemicals were purchased from Merck, Darmstadt, Germany.

PREPARATION OF GIANT UNILAMELLAR VESICLES

Dried lipid films containing 20 ng of lipids and 0.5% lipid-conjugated dyes were formed by drying lipid/dye chloroform solutions onto clean glass surfaces. GUVs were created by hydrating these films using sugar solutions (e.g. sucrose or galactose) at temperatures exceeding the chain melting temperature of the lipid mixtures. As DPPC possess the highest melting temperature of the lipids used in this study (41°C) (Yarrow et al., 2005), we conducted electroformation (Dimitrov and Angelova, 1987; Angelova et al., 1992) at 45°C to guarantee full fluidity of our lipid mixtures. Electroformation was conducted in a Vesicle Prep Pro chamber (Nan]i[on, Munich, Germany) fitted with conductive ITO glass slides, in which application of an AC current at 5 Hz and 3 V for 120 min produced GUVs of highly reproducible quality, yielding high abundance of 5–50 μm sized GUVs.

The selection of lipid mixtures was made on the basis of previously reported phase separation data, in the absence of

net osmotic gradients, at 23˚C (Veatch and Keller, 2003b). The chosen lipid mixtures enabled studies of systems comprising S_o/L_d domains (i.e., solid ordered/liquid ordered, referred to as "gel mixtures") or optically homogenous mixtures referred to as "raft mixtures," which have a propensity for L_o/L_d phase separation (i.e., liquid ordered/liquid disordered). The gel mixtures were composed of DOPC/DPPC and the raft mixtures based on POPC/sphingomyelin/cholesterol. Both types of mixtures were also examined when containing the ganglioside GM1.

IMAGING OF GIANT UNILAMELLAR VESICLES

5 or 10 μl aliquots of freely suspended membranes of sugar-encapsulating GUVs were studied at ambient temperature in eight-well chambers fitted with a coverslip bottom (Nunc, Rochester, USA). GUVs loaded with sugars readily sediment to the bottom of the chambers, facilitating long-term imaging of essentially immobilized GUVs close to the focal plane. We chose chambers over the conventional coverslip sandwiches for several reasons; (1) they reduce the risk of GUV deformation by mechanical pressure; (2) they afford large sample volumes, which reduces the possibility of inadvertent generation of significant osmotic imbalances due to solvent evaporation during extended experimental timescales (e.g., overnight); (3) they enable osmotic gradient generation in real-time; and (4) they allow solvent exchange, bilayer formation and even GUV formation directly inside the chamber. Osmotic gradients were produced by either exposing GUVs to a positive or negative concentration gradient, $\Delta C = ([\text{solute}]_{\text{outside}} - [\text{solute}]_{\text{inside}})$. *Positive* gradients were generated by adding appropriate volumes of solute solution, and *negative* ones by adding pure MilliQ water, to the external dispersion medium. Vesicles were monitored in real-time using wide-field deconvolution fluorescence microscopy. Imaging was conducted using a DeltaVision microscope (Applied Precision, Inc., WA, USA) fitted with a PLAPON 60XO/1.42 NA oil-immersion objective from Olympus, and DAPI, TRITC, FITC and CY5 Semrock filters (New York, USA). Images were processed using the ImageJ freeware (http://rsbweb.nih.gov/ij/) and the DeltaVision software Softworx 4.1.0.

RESULTS

FLUORESCENT PHASE MARKERS

By incorporation of phase-sensitive, amphiphilic fluorescent dyes into GUV membranes, we were able to image in-plane phase separation dynamics concomitantly with out-of-plane morphological changes induced by osmotic gradients. Rhodamine-DPPE (Rho-DPPE; a photostable, widely used L_d phase marker; Baumgart et al., 2003, 2007b; Juhasz et al., 2010) and Laurdan (Harris et al., 2002), an ordered phase marker, were used as reference dyes in both homogenous and phase separated lipid mixtures. A selection of the dyes' partitioning preferences in a gel-forming GUV consisting of equimolar DOPC and DPPC lipids is illustrated by the fluorescence images shown in **Figure 1**. These images confirm the phase-sensitive partitioning preferences of Laurdan and Rhodamine-DPPE and show that Atto488-DPPE (488-DPPE) colocalizes with Laurdan in gel-containing systems. By the same method, we established that 5-TAMRA-J116S and Rho-DOPE decorate the L_d phase.

IN-PLANE AND OUT-OF-PLANE MORPHOLOGICAL TRANSFORMATIONS IN HOMOGENOUS "RAFT MIXTURES"

In-plane phase separation in the presence of negative osmotic gradients

Establishing negative sugar gradients across GUV membranes (see Materials and Methods), causes inflation of the intravesicular space due to water influx. We found that various microscopically homogeneous membranes (i.e., POPC/sphingomyelin/cholesterol based mixtures) respond radically to the onset of negative osmotic gradients by forming raft-mimicking, cholesterol-, and sphingomyelin-enriched L_o domains in the L_d phase surroundings, consisting primarily of POPC. **Figure 2** shows an ensemble of GUVs composed of POPC:SM:Ch:GM1 (33:33:33:8), encapsulating 1 M sucrose under negative osmotic stress. The image reveals that individual vesicles display dramatically different phase separation characteristics ranging from optically homogeneous to various microscopic sizes of dye-enriched L_d phase domains. This variation of domain sizes is intriguing because the giant vesicles are likely to be of comparable compositions (within 5%). Moreover, osmolarity gradients are unlikely to initially vary across the

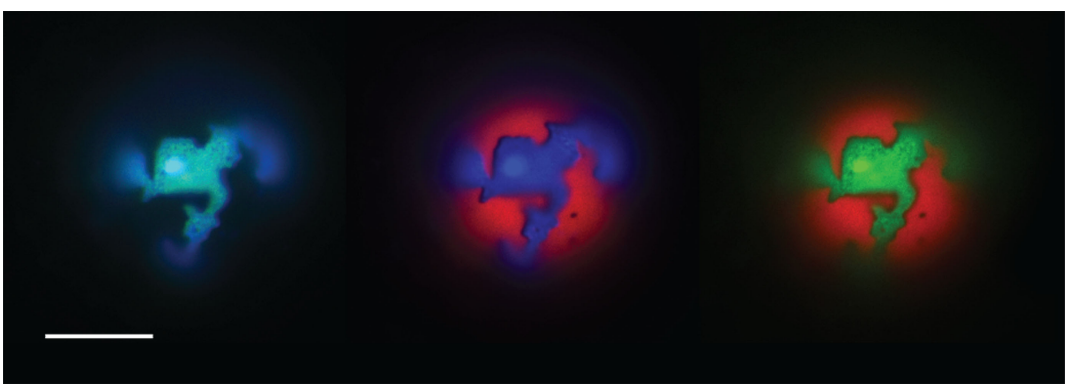

FIGURE 1 | The partitioning behavior of three amphiphilic dyes in a DOPC:DPPC (1:1) GUV entrapping 1 M sucrose. *Left* blue channel (Laurdan) and green cannel (488-DPPE) – both staining the S_o phase. *Center* red channel (Rho-DPPE) and green channel (488-DPPE) staining the L_d and S_o phase respectively. *Right* red channel (Rho-DPPE) and blue channel (Laurdan) staining the L_d and S_o phase respectively. Scale bar: 10 μm.

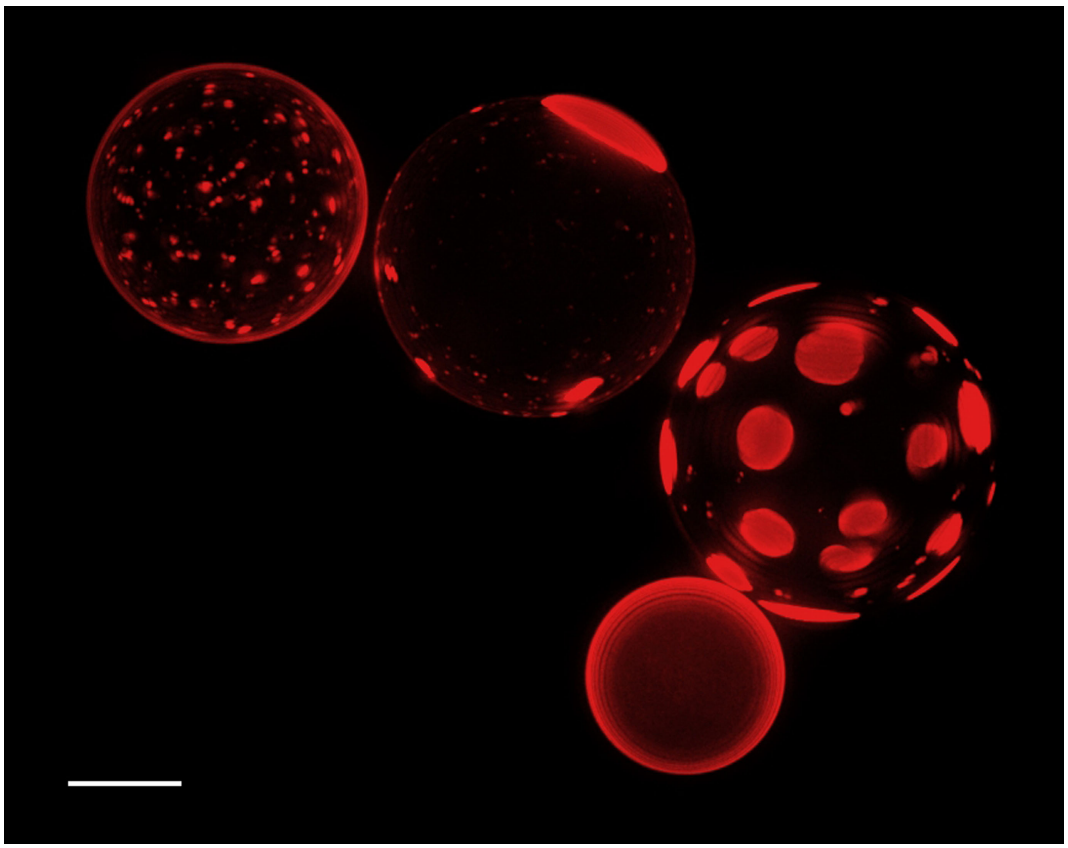

FIGURE 2 | The lower hemispheres of GUVs (deconvolved *Z*-stack) comprising POPC:SM:Ch:GM1 (33:33:33:8), which have been inflated by an osmotic stress at room temperature (1 M sucrose inside, MilliQ outside), are shown. No phase separation was observed prior to sample dilution in MilliQ water. 0.5 mol% Rho-DPPE was used to label the L_d phase. Scale bar: 10 μm.

vesicular population in single samples of large (5–50 μm) vesicles (Luisi et al., 2011). Based on these considerations, we deduce that the existence of the observed diversity in domain sizes must reflect a departure from the true equilibrium ground state, induced by the coupling of membrane phase separation (internal compositional degrees of freedom) with the osmotic and hydrodynamic forces generated due to the osmotic gradient.

In-plane phase separation in the presence of weak positive osmotic gradients

The sequence of epifluorescence images shown in **Figure 3** illustrates the dramatic shape change and a characteristic vesicle involution that result from the onset of weak positive osmotic gradients. The gradient was generated by adding 10 μl of 100 mM potassium phosphate buffer, pH 7.4, to the sample shown in **Figure 2**, after osmotic equilibration had been established. Salient features of the osmotically induced vesicular structural transformations brought out by these data are described in turn below. *First*, immediately following the creation of positive osmotic gradient, the spherical vesicles deform producing elongated prolate-like morphologies. This deflated structure matches earlier theoretical predictions (Deuling and Helfrich, 1976) and the so-called re-entrant transition reported by Berndl et al. (1990). It manifests the effect of curvature elasticity of vesicles under the conditions of the availability of excess membrane area, in our case, due to reduction in volume caused by efflux of water from the vesicular confinement. *Second*, an examination of the fluorescence pattern reveals an unusual extended phase separation pattern revealing a network of a fluorescence depleted rivulet-like phase in a strongly fluorescent background. In tense spherical vesicles, similar chemical compositions do not produce such extended domain morphologies. This indicates that the lateral phase separation is directly influenced by the macroscopic vesicular shape transformations, consistent with the expected coupling of elastic properties with local chemical compositions (Asciutto et al., 2005). Since the lipid-dye used has an affinity for the fluid phase, the dark rivulet-like structure can be ascribed to the L_o (or S_o) phase.

Despite their appearance, the shape characteristics of the branched, elongated domains of the discrete phase may indeed represent the L_o phase. Specifically, previous theoretical work predicts shape instability in phase-separating fluid systems resulting from competing interactions in constrained topologies (Seul and Andelman, 1995). This is because macroscopic equilibrium phase separation is expected when line tension is the sole determinant because it minimizes the phase boundary. In the presence of a competing repulsive interaction such as dipolar repulsion between molecules, the line tension effects are opposed, and modulated phases consisting of discrete domains (or stripes) appear

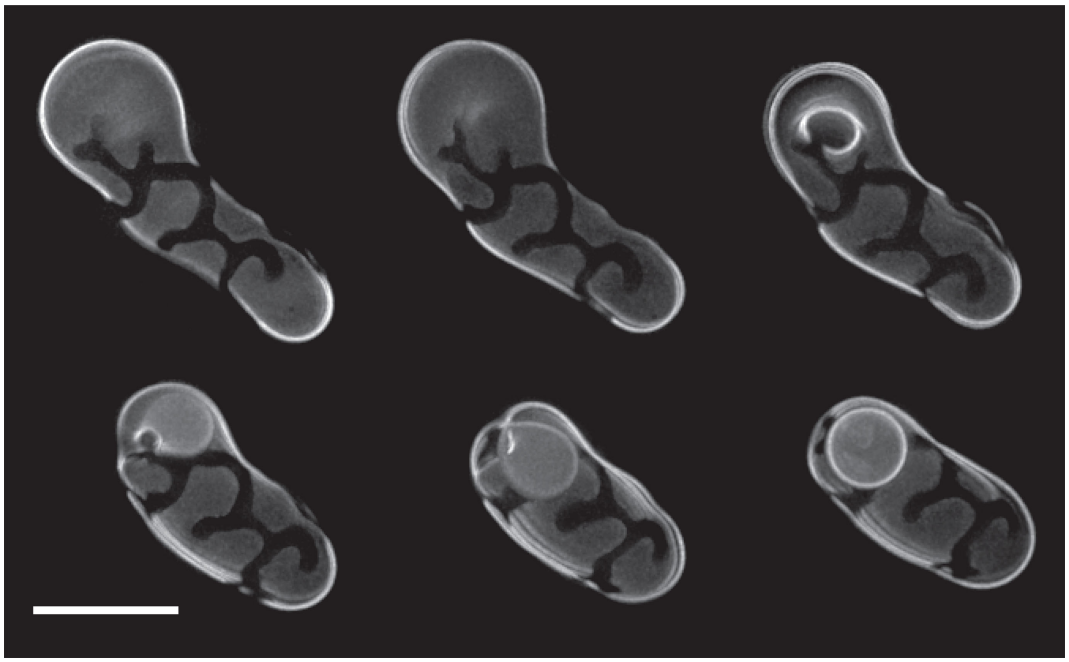

FIGURE 3 | A POPC:SM:Ch:GM1 (33:33:33:8) GUV undergoing deflation is shown in sequence. Deflation was induced by addition of 10 μl of 100 mM potassium phosphate buffer, pH 7.4, into the sample illustrated in **Figure 2**. Involution of the L_d phase (labeled with Rho-DPPE) resulted in the formation of an internalized daughter GUV. The image series shows the lower hemisphere of the vesicle (deconvolved *Z*-stack) at different time points. Scale bar: 10 μm.

and instabilities ensue (Seul and Andelman, 1995). One such instability occurs when circular domains become unstable to elliptical distortion, or when stripes rupture in constrained topologies (e.g., ellipsoidal phase space) producing branched domain structures such as we observe. Implicit in these observations is the unique property of raft phases in membranes, that they are not rigid, solid state domains. Rather, their essentially fluid character imparts to them the susceptibility to shape instabilities. Alternatively, the rivulet morphology we observe may represent S_o phase domains formed by reflecting an incipient phase change likely due to the topological constraints. Like the L_o phase, they exclude fluorescent markers that prefer disordered lipid phases. Moreover, they appear essentially immobile in long-term imaging. Because these characteristics may be shared by deformed L_o phases and S_o phases, we cannot conclusively differentiate between the two scenarios, L_o or S_o phase formation, for rivulet structures. The precise phase state of the rivulet structures notwithstanding, their emergence and extended character determined by their coupling to the macroscopic shape of the elastic membrane is notable.

Vesicle involution in the presence of weak positive osmotic gradients

The image series shown in **Figure 3** also illustrates a sequence of out-of-plane transformations observed in a single, deflating GUV. Water efflux creates negative intravesicular pressure, which leads to the involution of a daughter vesicle – in this case from the homogenous, L_d (Rho-DPPE-labeled) phase of the mother membrane. Concomitantly with the vesiculation, we observe shrinkage of the mother vesicle area (see Video S1 in Supplementary Material). The rate and onset of involution depends on the strength of the osmotic gradient, ranging between seconds to minutes.

Involution occurs in raft mixtures regardless of their state of phase separation. In **Figure 4**, initially inflated POPC:SM:Ch:GM1 (45:30:25:8) GUVs encapsulating saturated galactose solution, have been rendered floppy by the addition of 5 μl of 1 M sucrose solution to the sample bulk. The positive osmotic gradient so created is manifest in the deflated morphologies that result. Moreover, the images reveal the sequential production of involuted daughter vesicles. It is instructive to note that since daughter vesicles are formed via membrane inclusion, their interiors at first encapsulate the ambient bulk. This results in the osmotic gradient across the daughter membranes being initially identical, but inverted, to the gradient across the mother vesicle membrane. This inversion is also reflected in their tense boundaries immediately after involution and an accompanying onset of phase separation. This contrasts with the non-phase separated, homogeneous character of the daughter vesicles in **Figure 3**. These two cases present an interesting contrast, wherein heterogeneity in the daughter vesicle is induced from the homogeneous mother, by virtue of re-introduction of an osmotic gradient in the reverse direction in **Figure 4**. Conversely, in **Figure 3**, a heterogeneous mother vesicle gives rise to a homogenous daughter, again via inversion.

Taken together, the appearance of dynamic processes, illustrated in **Figures 3** and **4**, indicate that prominent out-of-plane transitions, reminiscent of endocytosis, can be induced in membranes of arbitrary compositions, simply by the introduction of osmotic gradients. These transformations also create topologically

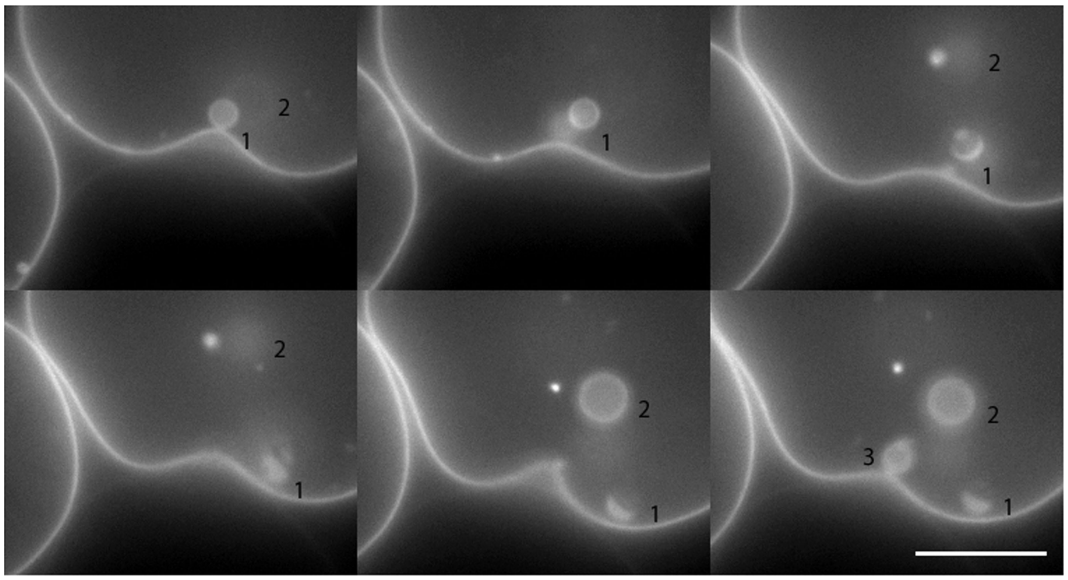

FIGURE 4 | Still images of daughter vesicle internalization resulting from negative intravesicular pressure in a POPC:SM:Ch:GM1 (45:30:25:8) GUV induced by the addition of 5 μl of 1 M sucrose to the aqueous (205 μl) bulk of a previously inflated GUV population. The formed daughter vesicles are numbered in the images series for tracking purposes. Scale bar: 10 μm.

and biochemically distinct daughter vesicles with different interiors and with membrane compositions that may mirror or become different from their parent sources.

Direct expulsion induced by negative osmotic gradients

Another remarkable phenomenon induced by negative osmotic gradients – direct expulsion of intact internal vesicles – is illustrated in the image series of **Figure 5**. Here, a "vesosome" (a vesicle containing internalized vesicles), composed of POPC:SM:Ch:GM1 (45:30:25:8) and loaded with a saturated galactose solution, is seen to expel an internal vesicle to the ambient bulk. As a consequence of the negative osmotic gradient and attendant water influx, intravesicular pressure rises in all vesicles of the vesosomal structure. This internal hydrodynamic pressure as well as the mechanical pressure created by internal crowding within the GUV, we reason, triggers a dramatic translocation of the entire intact vesicle. Such translocation requires a transiently formed pore in the entrapping GUV membrane, which must dilate to accommodate the exiting vesicle while concomitantly deforming the expelled GUV (presumably due to the constraint placed on pore expansion by the sudden drop in intravesicular pressure caused by substantial volume loss). Upon complete expulsion, the spherical shape of the daughter vesicle is immediately recovered and instant healing of the transient pore can readily be observed (see Video S2 in Supplementary Material). Subsequently, all vesicles continue to gain volume, as an osmotic gradient is still in place. The extraordinary observation is that large microscopic pore formation – under certain circumstances – is favored over membrane fusion despite significant pressure being applied to all three vesicles. Direct expulsion is however not contingent on internal vesicle crowding and has been observed to be induced by hydrodynamic pressure alone (data not shown).

MORPHOLOGICAL TRANSFORMATIONS IN PHASE SEPARATED "GEL MIXTURES" SUBJECTED TO OSMOTIC STRESS

The dynamics of osmotically induced phase separation and membrane morphology in gel-forming (fluid–solid) mixtures (i.e., DOPC/DPPC based mixtures) differ substantially from those of POPC/sphingomyelin/cholesterol based mixtures. Phase separation in gel-forming mixtures is present in the absence of osmotic gradients at room temperatures. This is not surprising since the S_o phase is immiscible with the surrounding fluid phase. Upon osmotic inflation and/or deflation the S_o phase domains do not coalesce (see Video S3 in Supplementary Material, showing the fine details of the S_o network in a DOPC:DPPC:GM1 (1:1:1) GUV entrapping 1 M sucrose, with a resolution below 0.5 μm). As a consequence of its S_o character, osmotic deflation of GUV containing gel-forming lipids, produces protrusions (both inward and outward) in response to diminishing GUV volume. The protrusions appear to be composed primarily of the L_d phase. The "rigid cage" composed of the S_o phase tightens around the fluid background, forcing excess L_d membrane to flex, as seen in the DOPC:DPPC (1:1) GUVs shown in **Figure 6A**. In many cases, these cylindrical protrusions become unstable, producing twisted rope-like morphologies. Inflation, on the other hand, produces perfectly spherical GUVs with rigid S_o rivulets on a fluid L_d background (**Figure 6B**, showing a DOPC:DPPC:GM1 (1:1:1) containing 1 M sucrose).

OSMOTICALLY INDUCED CYLINDRICAL DEFORMATIONS AND THEIR TRANSITION TO PEARLED STATES

Previous studies have documented another common shape deformation in which excess vesicle area gives rise to cylindrical tubule formation and their subsequent transformation into pearling states. The excess area is variously produced by exploiting differences in thermal expansivities of the membrane leaflets (and of

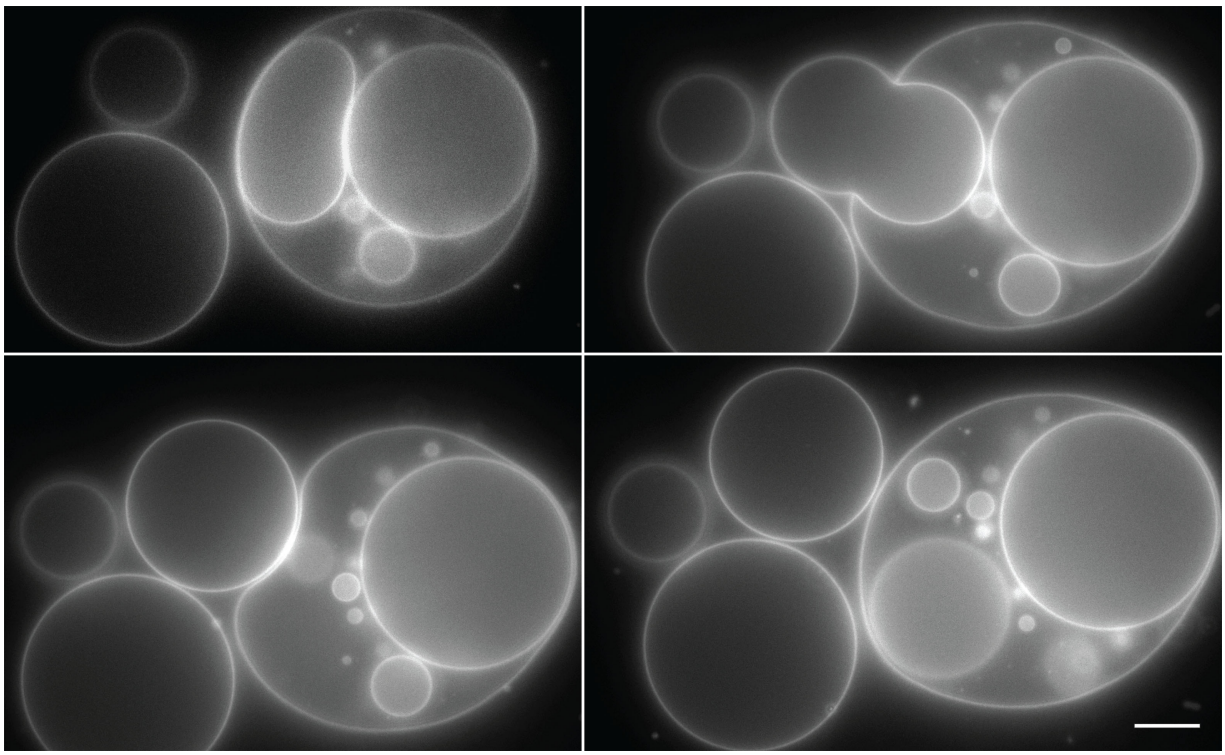

FIGURE 5 | Direct expulsion of internalized GUV through a transient pore. POPC:SM:Ch:GM1 (45:30:25:8) GUVs, loaded with a saturated galactose solution, were diluted with MilliQ water to establish an osmotic gradient. The GUVs were stained with Rho-DPPE and imaged at room temperature. Scale bar: 10 μm.

water; Boroske et al., 1981) or by exogenously applying pressure using laser tweezers (Bar-Ziv and Moses, 1994) or nanoparticle adhesion (Yu and Granick, 2009). We observed these kinds of transitions under shifting osmotic gradients. **Figure 7** illustrates one such transition. Here, Rho-DOPE labeled (0.5%) egg PC GUVs encapsulating 300 mM sucrose and 100 μM fluorescein were diluted with MilliQ water. The onset of pearling began 45 min after the introduction of the gradient and took place on a time scale of seconds. We surmise that the late-stage tubulation and pearling corresponds to the reversal of the osmotic gradient as osmotically equilibrated GUV samples that are allowed to lose ambient water through evaporation (and thus increase the solute concentration in the ambient surrounding) will experience a weak, positive osmotic gradient.

VESICLE RUPTURE AND MEMBRANE FUSION IN THE PRESENCE OF IONS

The presence of ions in the hydration solvent (e.g., by buffers or $CaCl_2$) during GUV formation hampers overall GUV formation regardless of the preparation method used. When using raft mixtures, nested vesicles, GUV clusters as well as bilayer formation is frequently encountered. Tubulation often occurs during spontaneous formation, which is believed to be an effect of hydrodynamic flow (Yuan et al., 2008). Moreover, we repeatedly observe membrane merger between neighboring and/or internal GUVs as a way to accommodate an increasing vesicle volume during inflation perpetuated by negative osmotic pressure (data not shown). Another common outcome in these systems is GUV rupture, as GUVs entrapping ions are unable to rapidly reach osmotic equilibrium by diffusion of ions across the lipid bilayer. This event is always followed by supported bilayer formation.

DISCUSSION

In this study, we subjected model GUV membranes to ionic and non-ionic osmotic gradients. The GUVs we used consisted of a variety of multicomponent lipid mixtures, which produce coexisting fluid–fluid (L_d/L_o) or fluid–gel (L_d/S_o) phases. The effects of both positive and negative osmotic gradients were investigated. Using a sensitive CCD camera and wide-field fluorescence deconvolution microscopy, we were able to image osmotically induced in-plane and out-of-plane membrane deformations over extended periods of time without inflicting apparent photo-oxidation of lipids (Yuan et al., 2008). Under these conditions, a host of macroscopic membrane modulations were captured "in the act" of vesiculation, fingering, tubulation, "pearling," raft formation, as well as direct expulsion of intact vesicles. We found that vesicle morphologies can be drastically altered in the presence of even weak osmotic gradients that arise from as little as 5 mM difference in solute concentration across the membrane. Precise strengths and direction of the imposed osmotic gradient and details of membrane chemical composition determine the types of deformations that ensue. Previously, comparable membrane deformations have been reported in GUVs by utilizing temperature as sources of external perturbations (Veatch and Keller,

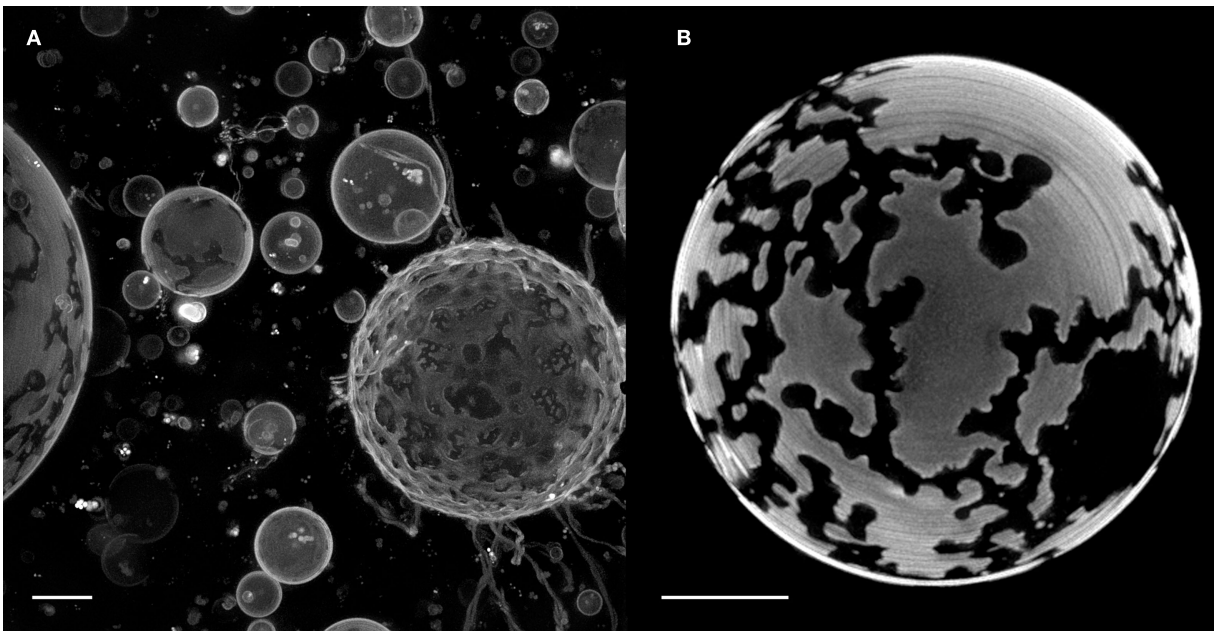

FIGURE 6 | Giant unilamellar vesicles composed of DOPC:DPPC (1:1) exhibit So/Ld phase separation regardless of the presence or absence of osmotic gradients. Experiments were performed at room temperature, at which separation was stable over the full time course of imaging. **(A)** Deflation of DOPC:DPPC (1:1) GUVs encapsulating 1 M sucrose was accomplished by adding 10 μl of 100 mM potassium phosphate buffer, pH 7.4, to an inflated GUV population. The disordered phase was labeled with 0.5% of the lipid analog 5-TAMRA-J116S. The image shows a deconvolved *Z*-stack of the whole vesicles. **(B)** An inflated DOPC:DPPC:GM1 (1:1:1) GUV, entrapping 1M sucrose, after swelling by addition of MilliQ water. The L_d phase was stained with 0.5% Rho-DPPE. (Adobe Photoshop was used for the cosmetic removal of out-of-plane artifacts that would have obstructed the view of the details of interest). Image shows a deconvolved *Z*-stack of the bottom hemisphere. Scale bars: 10 μm.

2003a, 2005a,b; Veatch et al., 2006; Sakuma and Imai, 2011) or pH (Khalifat et al., 2008). It has also been shown that similar deformations can also be achieved by altering the membrane composition by incorporation of curvature-inducing sterols (Bacia et al., 2005) or selective solubilization using detergent interactions (Staneva et al., 2005; Muddana et al., 2012).The ability of osmotic gradients to reproduce large-scale membrane deformations suggests how physicochemical processes, that underscore spatio-temporal membrane organization, can be modulated by coupling with osmotic gradients to produce complex behaviors.

The morphological transformations we observed under negative and positive osmotic stress in GUVs of fluid composition, i.e., 2D phase separation into ordered domains, have previously been observed only under conditions that shift the compositional requirement for a phase transition point, for example by lowering the temperature (Baumgart et al., 2007a; Veatch et al., 2008; Uline et al., 2012). In non-phase separated mixtures, negative gradients gave rise to phase separation that proceeded with different kinetics, apparently dependent upon vesicle diameter, as evidenced by the variety of different domain sizes that could be observed in a single field of vesicles. Since no change in composition occurs in these GUVs during the observation time (by fission or fusion), we can hypothesize that internal pressure that inflates the vesicle thereby exerts a force on the membrane that effectively substitutes for a decrease in temperature. The effects of pressure on phase separation are currently under investigation in our lab in more detail.

When deflating the above mentioned sample by an ionic osmotic gradient, more rigid domains formed, which appeared to force the remaining fluid regions of the membrane to involute and reduce the total membrane volume.

Vesicle fusions observed upon inflation of GUVs in the presence of ions, are highly reminiscent of certain cellular behaviors that have been documented, or postulated to occur during membrane trafficking between cellular compartments. For example, formation of the autophagosome, a double-membraned vesicular organelle responsible for degradation of cytoplasmic contents and aged organelles (Levine and Kroemer, 2009), is thought to originate at the endoplasmic reticulum (ER) membrane, via protrusion of membrane "flanges" which ultimately engulf an enclosed space. It is known that autophagy can be induced by calcium released from the ER lumen after induction by various agents (Harris et al., 2002). With regard to our observations, local calcium gradients across the ER membrane would be an interesting explanation if indeed local osmotic gradients of ions such as calcium could provide an initial driving force for the extreme membrane bending and fusion that is required to produce such compartments.

Other unconventional membrane transformations and exchanges ("heterotypic contacts") have been proposed, e.g., that between mitochondria and the ER (Fagone and Jackowski, 2009; Chipuk et al., 2012), in addition to the more established membrane contact sites between different compartments, like that between ER and the nuclear membrane, or Golgi vesicles (van Meer and Sprong, 2004; Holthuis and Levine, 2005). Lipid exchange is

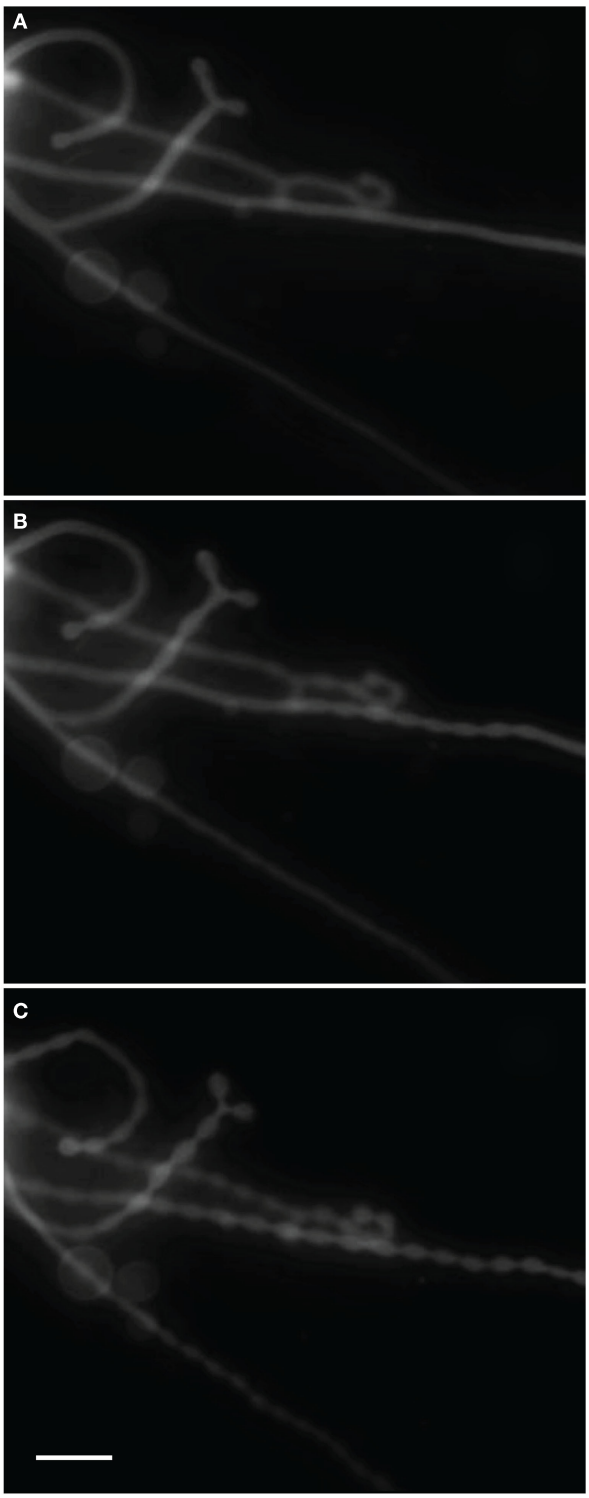

FIGURE 7 | Time series of Rho-DOPE stained (0.5%) POPC GUVs encapsulating 300 mM sucrose and 100 μM fluorescein diluted with MilliQ water. Pearling of hollow tubes initiated after 45 min of incubation, presumably after the inversion of the osmotic gradient as a result of solute equilibration followed by sample evaporation. **(A)** Tubes just prior to the onset of pearling. **(B)** Intermediary tube-pearl state after 6 s. **(C)** Pearled state after 23 s. Scale bar: 20 μm.

thought to occur at these points, although the mechanisms have not been fully established. The effects of local osmotic gradients, such as described here, might generate physical conditions which foster close approach of these heterotypic membranes facilitating molecular exchange by transient membrane-membrane fusion. Indeed, fusion of vesicles was one of the behaviors that we observed to be triggered by negative osmotic stress.

Finally, membrane protrusions like those observed in gel-forming mixtures under positive osmotic stress we suggest are reminiscent of the finger-like projections that have been proposed to occur at non-ordered regions of the plasma membrane (Goswami et al., 2008). It may be that osmotic stress possibly introduced by ion flows could play a role in giving an impetus to the formation of such membrane protrusions.

While a wide range of membrane compositions under the influence of osmotic gradients are clearly capable of undergoing surprisingly varied and extreme morphological behaviors in both 2D and 3D, membranes that bound real-world cellular compartments do so under the influence of a complex array of accessory proteins. In a pre-biotic era, however, it may have been the case that osmotic gradients provided sufficient force to create relatively complex membrane-bound compartments that might have given a thermodynamic advantage to any proto-cell that created them, for example by entrapping simple organic molecules in a confined space. Whether or not this actually happened, we propose that osmotic gradients could at least give an impetus that would be capable of kick-starting membrane trafficking and vesiculation events even in modern cells.

ACKNOWLEDGMENTS

We are grateful to Dr. Jaume Torres for the usage of the Nan]i[on electroformation chamber for GUV preparations, and to Dr. Gary Jennings and Jado-Tech for the J116S dye. This research was supported by the AcRF Tier II grant, grant number MOE2009-T2-2-019. Work at UC Davis was supported by a grant from Biomolecular Materials Program, Division of Materials Science and Engineering, U.S. Department of Energy under award number DE-FG02-04ER46173.

SUPPLEMENTARY MATERIAL

The Video S1, S2, and S3 for this article can be found online at: http://www.frontiersin.org/Membrane_Physiology_and_Biophysics/10.3389/fphys.2012.00120/abstract

Video S1 | Video of Figure 3; A POPC:SM:Ch:GM1 (33:33:33:8) GUV undergoing deflation induced by addition of 10 μl of 100 mM potassium phosphate buffer, pH 7.4 into the sample illustrated in Figure 2. Involution of the L_d phase results in the formation of an internalized GUV. The image series show the bottom hemisphere of the vesicle (deconvolved *Z*-stack). Scale bar: 10 μm.

Video S2 | Video of Figure 5; direct expulsion of an internalized GUV through a transient pore. POPC:SM:Ch:GM1 (45:30:25:8) GUVs, loaded with a saturated galactose solution, were diluted with MilliQ water to establish an osmotic gradient. The GUVs were stained with Rho-DPPE and imaged at room temperature. Scale bar: 10 μm.

Video S3 | A DOPC:DPPC:GM1 (1:1:1) GUV, labeled with Rho-DPPE was loaded with 1 M sucrose and subjected to an negative osmotic gradient to induce swelling. The video illustrates the rigidity of S_o domains and serves as a comparison to the dynamics of the dark rivulets shown in video S1.

REFERENCES

Angelova, M. I., Soléau, S., Méléard, P., Faucon, J. E., and Bothorel, P. (1992). Preparation of giant vesicles by external AC electric fields. Kinetics and applications. *Prog. Colloid Polym. Sci.* 89, 127–131.

Asciutto, E., Roland, C., and Sagui, C. (2005). Self-assembled patterns and strain-induced instabilities for modulated systems. *Phys. Rev. E Stat. Nonlin. Soft Matter Phys.* 72, 021504.

Bacia, K., Schwille, P., and Kurzchalia, T. (2005). Sterol structure determines the separation of phases and the curvature of the liquid-ordered phase in model membranes. *Proc. Natl. Acad. Sci. U.S.A.* 102, 3272–3277.

Bar-Ziv, R., and Moses, E. (1994). Instability and "pearling" states produced in tubular membranes by competition of curvature and tension. *Phys. Rev. Lett.* 73, 1392–1395.

Baumgart, T., Hammond, A. T., Sengupta, P., Hess, S. T., Holowka, D. A., Baird, B. A., and Webb, W. W. (2007a). Large-scale fluid/fluid phase separation of proteins and lipids in giant plasma membrane vesicles. *Proc. Natl. Acad. Sci. U.S.A.* 104, 3165–3170.

Baumgart, T., Hunt, G., Farkas, E. R., Webb, W. W., and Feigenson, G. W. (2007b). Fluorescence probe partitioning between Lo/Ld phases in lipid membranes. *Biochim. Biophys. Acta* 1768, 2182–2194.

Baumgart, T., Hess, S. T., and Webb, W. W. (2003). Imaging coexisting fluid domains in biomembrane models coupling curvature and line tension. *Nature* 425, 821–824.

Berndl, K., Käs, J., Lipowsky, R., Sackmann, E., and Seifert, U. (1990). Shape transformations of giant vesicles – extreme sensitivity to bilayer asymmetry. *Europhys. Lett.* 13, 659–664.

Bloom, M., Evans, E., and Mouritsen, O. G. (1991). Physical properties of the fluid lipid-bilayer component of cell membranes: a perspective. *Q. Rev. Biophys.* 24, 293–397.

Boroske, E., Elwenspoek, M., and Helfrich, W. (1981). Osmotic shrinkage of giant egg-lecithin vesicles. *Biophys. J.* 34, 95–109.

Budin, I., and Szostak, J. W. (2011). Physical effects underlying the transition from primitive to modern cell membranes. *Proc. Natl. Acad. Sci. U.S.A.* 108, 5249–5254.

Chipuk, J. E., Mcstay, G. P., Bharti, A., Kuwana, T., Clarke, C. J., Siskind, L. J., Obeid, L. M., and Green, D. R. (2012). Sphingolipid metabolism cooperates with BAK and BAX to promote the mitochondrial pathway of apoptosis. *Cell* 148, 988–1000.

Deamer, D. W., and Bramhall, J. (1986). Permeability of lipid bilayers to water and ionic solutes. *Chem. Phys. Lipids* 40, 167–188.

Deuling, H. J., and Helfrich, W. (1976). The curvature elasticity of fluid membranes: a catalogue of vesicle shapes. *J. Phys.* 37, 1335–1345.

Dimitrov, D. S., and Angelova, M. I. (1987). Lipid swelling and liposome formation on solid surfaces in external electric fields. *Prog. Colloid Polym. Sci.* 73, 48–56.

Döbereiner, H. G., Evans, E., Kraus, M., Seifert, U., and Wortis, M. (1997). Mapping vesicle shapes into the phase diagram: a comparison of experiment and theory. *Phys. Rev. E* 55, 4458–4474.

Döbereiner, H. G., Käs, J., Noppl, D., Sprenger, I., and Sackmann, E. (1993). Budding and fission of vesicles. *Biophys. J.* 65, 1396–1403.

Evans, E., and Needham, D. (1987). Physical properties of surfactant bilayer membranes: thermal transitions, elasticity, rigidity, cohesion, and colloidal interactions. *J. Phys. Chem.* 91, 4219–4228.

Fagone, P., and Jackowski, S. (2009). Membrane phospholipid synthesis and endoplasmic reticulum function. *J. Lipid Res.* 50, S311–S316.

Fournier, J. B., Khalifat, N., Puff, N., and Angelova, M. I. (2009). Chemically triggered ejection of membrane tubules controlled by intermonolayer friction. *Phys. Rev. Lett.* 102, 018102.

Frolov, V. A., Shnyrova, A. V., and Zimmerberg, J. (2011). Lipid polymorphisms and membrane shape. *Cold Spring Harb. Perspect. Biol.* 3. doi: 10.1101/cshperspect.a004747

Goswami, D., Gowrishankar, K., Bilgrami, S., Ghosh, S., Raghupathy, R., Chadda, R., Vishwakarma, R., Rao, M., and Mayor, S. (2008). Nanoclusters of GPI-anchored proteins are formed by cortical actin-driven activity. *Cell* 135, 1085–1097.

Harris, F. M., Best, K. B., and Bell, J. D. (2002). Use of laurdan fluorescence intensity and polarization to distinguish between changes in membrane fluidity and phospholipid order. *Biochim. Biophys. Acta* 1565, 123–128.

Holthuis, J. C., and Levine, T. P. (2005). Lipid traffic: floppy drives and a superhighway. *Nat. Rev. Mol. Cell Biol.* 6, 209–220.

Juhasz, J., Davis, J. H., and Sharom, F. J. (2010). Fluorescent probe partitioning in giant unilamellar vesicles of "lipid raft" mixtures. *Biochem. J.* 430, 415–423.

Käs, J., and Sackmann, E. (1991). Shape transitions and shape stability of giant phospholipid vesicles in pure water induced by area-to-volume changes. *Biophys. J.* 60, 825–844.

Khalifat, N., Puff, N., Bonneau, S., Fournier, J. B., and Angelova, M. I. (2008). Membrane deformation under local pH gradient: mimicking mitochondrial cristae cynamics. *Biophys. J.* 95, 4924–4933.

Koslov, M. M., and Markin, V. S. (1984). A theory of osmotic lysis of lipid vesicles. *J. Theor. Biol.* 109, 17–39.

Levine, B., and Kroemer, G. (2009). Autophagy in aging, disease and death: the true identity of a cell death impostor. *Cell Death Differ.* 16, 1–2.

Lipowsky, R. (1991). The conformation of membranes. *Nature* 349, 475–481.

Luisi, P. L., Allegretti, M., Pereira De Souza, T., Steiniger, F., Fahr, A., and Stano, P. (2011). Spontaneous protein crowding in liposomes: a new vista for the origin of cellular metabolism. *Chembiochem* 11, 1989–1992.

Martinac, B., Buechner, M., Delcour, A. H., Adler, J., and Kung, C. (1987). Pressure-sensitive ion channel in *Escherichia coli*. *Proc. Natl. Acad. Sci. U.S.A.* 84, 2297–2301.

Miao, L., Seifert, U., Wortis, M., and Döbereiner, H. G. (1994). Budding transitions of fluid-bilayer vesicles: the effect of area-difference elasticity. *Phys. Rev. E Stat. Phys. Plasmas Fluids Relat. Interdiscip. Topics* 49, 5389–5407.

Muddana, H. S., Chiang, H. H., and Butler, P. J. (2012). Tuning membrane phase separation using nonlipid amphiphiles. *Biophys. J.* 102, 489–497.

Needham, D., and Nunn, R. S. (1990). Elastic deformation and failure of lipid bilayer membranes containing cholesterol. *Biophys. J.* 58, 997–1009.

Sakuma, Y., and Imai, M. (2011). Model system of self-reproducing vesicles. *Phys. Rev. Lett.* 107, 198101.

Sandre, O., Moreaux, L., and Brochard-Wyart, F. (1999). Dynamics of transient pores in stretched vesicles. *Proc. Natl. Acad. Sci. U.S.A.* 96, 10591–10596.

Seifert, U. (1997). Configurations of fluid membranes and vesicles. *Adv. Phys.* 46, 13–137.

Seul, M., and Andelman, D. (1995). Domain shapes and patterns: the phenomenology of modulated phases. *Science* 267, 476–483.

Staneva, G., Seigneuret, M., Koumanov, K., Trugnan, G., and Angelova, M. I. (2005). Detergents induce raft-like domains budding and fission from giant unilamellar heterogeneous vesicles: a direct microscopy observation. *Chem. Phys. Lipids* 136, 55–66.

Uline, M. J., Schick, M., and Szleifer, I. (2012). Phase behavior of lipid bilayers under tension. *Biophys. J.* 102, 517–522.

van Meer, G., and Sprong, H. (2004). Membrane lipids and vesicular traffic. *Curr. Opin. Cell Biol.* 16, 373–378.

Veatch, S. L., Cicuta, P., Sengupta, P., Honerkamp-Smith, A., Holowka, D., and Baird, B. (2008). Critical fluctuations in plasma membrane vesicles. *ACS Chem. Biol.* 3, 287–293.

Veatch, S. L., Gawrisch, K., and Keller, S. L. (2006). Closed-loop miscibility gap and quantitative tie-lines in ternary membranes containing diphytanoyl PC. *Biophys. J.* 90, 4428–4436.

Veatch, S. L., and Keller, S. L. (2003a). A closer look at the canonical "Raft Mixture" in model membrane studies. *Biophys. J.* 84, 725–726.

Veatch, S. L., and Keller, S. L. (2003b). Separation of liquid phases in giant vesicles of ternary mixtures of phospholipids and cholesterol. *Biophys. J.* 85, 3074–3083.

Veatch, S. L., and Keller, S. L. (2005a). Miscibility phase diagrams of giant vesicles containing sphingomyelin. *Phys. Rev. Lett.* 94, 148101.

Veatch, S. L., and Keller, S. L. (2005b). Seeing spots: complex phase behavior in simple membranes. *Biochim. Biophys. Acta* 1746, 172–185.

Walde, P., Cosentino, K., Engel, H., and Stano, P. (2010). Giant vesicles: preparations and applications. *Chembiochem* 11, 848–865.

Yang, X. C., and Sachs, F. (1989). Block of stretch-activated ion channels in *Xenopus* oocytes by gadolinium and calcium ions. *Science* 243, 1068–1071.

Yarrow, F., Vlugt, T. J. H., van der Eerden, J. P. J. M., and Snel, M. M. E. (2005). Melting of a DPPC lipid bilayer observed with atomic force microscopy and computer simulation. *J. Cryst. Growth* 275, e1417–e1421.

Yu, Y., and Granick, S. (2009). Pearling of lipid vesicles induced by nanoparticles. *J. Am. Chem. Soc.* 131, 14158–14159.

Yuan, J., Hira, S. M., Strouse, G. F., and Hirst, L. S. (2008). Lipid bilayer discs and banded tubules: photoinduced lipid sorting in ternary mixtures. *J. Am. Chem. Soc.* 130, 2067–2072.

Zhelev, D. V., and Needham, D. (1993). Tension-stabilized pores in giant vesicles: determination of pore size and pore line tension. *Biochim. Biophys. Acta* 1147, 89–104.

Conflict of Interest Statement: The authors declare that the research was conducted in the absence of any commercial or financial relationships that could be construed as a potential conflict of interest.

Received: 14 March 2012; paper pending published: 04 April 2012; accepted: 11 April 2012; published online: 04 May 2012.

Citation: Oglęcka K, Sanborn J, Parikh AN and Kraut RS (2012) Osmotic gradients induce bio-reminiscent morphological transformations in giant unilamellar vesicles. Front. Physio. ***3****:120. doi: 10.3389/fphys.2012.00120*

This article was submitted to Frontiers in Membrane Physiology and Biophysics, a specialty of Frontiers in Physiology.